

Analog simulations of stochastic resonance

Ting Zhou* and Frank Moss

Department of Physics, University of Missouri at St. Louis, St. Louis, Missouri 63121

(Received 18 October 1989)

The term *stochastic resonance* has been adopted to describe an interesting statistical property of periodically modulated and noise-driven multistable dynamical systems: Under the proper conditions, an increase in the input noise level results in an increase in the output signal-to-noise ratio. That is, increasing the disorder of the input leads to increasing the order of the output. This curious phenomenon was first introduced as a possible explanation of the observed periodicity in the recurrences of the earth's ice ages. The phenomenon is, however, observable in a variety of devices ranging from lasers to electronic circuits. We present here the results of some analog simulations based on the simplest generic nonlinearity: the quartic bistable potential modulated with an additive sinusoidal function. These results are compared to recent theories where available. Special features of the power spectrum are observed, which are predicted by some but not all theories, and which are observed also in recent laser experiments. In addition to measurements of the power spectrum, upon which nearly all previous studies have been based, we introduce precision measurements of the probability density of residence times for which no nonadiabatic theory exists.

I. INTRODUCTION

The statistical phenomenon, characteristic of noise-driven, multistable systems, which has become known as *stochastic resonance*, was first introduced by Benzi, Sutera, and Vulpiani.¹ It is a property most often observed in periodically modulated, bistable, noise-driven systems, whereby the signal-to-noise ratio of the response passes through a maximum as some externally applied noise level is increased from zero. The response is usually defined as a switching event that carries the system from the neighborhood of one stable state to another. In the absence of periodic modulation, often called "the signal," such switching events are purely random. However, in the presence of the modulation they become more or less correlated with it. At both low and high intensities of the external noise, the modulation and the switching events are not well correlated, but at some intermediate value, i.e., at "resonance," they become better correlated. Obviously, such a characteristic property is of interest in analyses of the generalized switching process, especially within the context of information theory, but its first application was to global climate dynamics.

In 1982, Nicolis² and Benzi *et al.*³ suggested that stochastic resonance might account for the observed periodicity in the recurrences of the earth's ice ages. In that view, the earth's climate is represented by a one-dimensional bistable system, one stable state of which is a largely ice-covered earth.⁴ The external noise is assumed to derive from short-term fluctuations in the balance between radiative and transport processes, and the periodic modulation is most often supposed to originate from variations in the insolation resulting from a small, observed oscillation with a 100 000-year period in the eccentricity of the Earth's orbit.^{2,3} The first realization of stochastic resonance in a laboratory experiment was provided in 1983 by Fauve and Heslot, who periodically modulated

an electronic Schmitt trigger while applying white noise.⁵ This circuit behaves approximately like an idealized two-state system. These authors measured the power spectrum of the output of the switch for various levels of input noise intensity while the amplitude of the periodic modulation or "input signal" was held constant. From these measurements, they constructed the signal-to-noise ratio (SNR), which has now become the most frequently studied quantity, and they observed an increase of better than a factor of 5 in the SNR at the resonant value of the noise voltage. This experiment seems to have been largely ignored until quite recently.

Renewed interest in stochastic resonance has recently been stimulated by Vemuri and Roy who observed the effect in a ring laser operated as a bistable system.⁶ The bistability derives from a degeneracy in the direction of travel of the optic wave around the cavity. As the pump intensity passes through the lasing threshold, this direction at first switches randomly, driven by the intrinsic quantum noise, but then settles into one of the stable directions above threshold. The two directional states can thus be described by two potential wells separated by a barrier. Switching can be induced by modulating alternately the depths of the wells relative to the barrier with either noise and/or a periodic signal of sufficient amplitude. In the experiments of Vemuri and Roy, this modulation was introduced by means of an acousto-optic modulator placed within the cavity. The input to the modulator was the sum of a periodic signal and white noise. The resulting switching events were observed by monitoring a fraction of the beam intensity traveling in one direction. These authors measured the SNR of the beam switching signal as the noise intensity at the input of the acousto-optic modulator was varied. They observed all the features which had been previously observed with the Schmitt trigger plus a number of new ones. It is important to note that, unlike the theoretical

treatments and the simulations described below which were carried out for simple one-dimensional systems, the dye laser is at least two dimensional. Stochastic models of such higher-dimensional systems present problems which are not yet satisfactorily solved analytically. Therefore Vemuri and Roy compared their experimental data with digital simulations of the two-dimensional semiclassical laser equations. That their data were in quite good agreement with the digital simulations stands as a unique and possibly quite stringent test of these laser equations, since the application of wide-bandwidth noise stimulates virtually the entire range of possible dynamical behaviors. Moreover, the periodic modulation introduces a known time scale against which the inherent, characteristic times, as they appear in the equations, can be clocked.

The demonstration of stochastic resonance in the ring laser stimulated a large amount of recent theoretical activity⁷⁻¹¹ and two analog simulations.^{12,13} Nearly all of these studies focused on the simple, one-dimensional, bistable potential

$$U(x) = - \left[\frac{a}{2} \right] x^2 + \left[\frac{b}{4} \right] x^4 - cx \sin(\omega_m t), \quad (1.1)$$

where a , b , and c are parameters, and ω_m is the modulation frequency. When noise $V_n(t)$ is added, the corresponding Langevin equation in the limit of large damping is

$$\dot{x} = ax - bx^3 + c \sin(\omega_m t) + V_n(t). \quad (1.2)$$

In addition, in Ref. 7 an idealized two-state model was considered, wherein the dynamics given by Eq. (1.2) was filtered in such a way that the only relevant output information is the well wherein the trajectory is found. In this paper, we shall call this the filtered two-state dynamics. Moreover, in the analog simulation of Ref. 12 some data for a damped oscillator were presented. Most theoretical studies have considered Gaussian noise in the white noise limit [see, however, Ref. 12(b)],

$$\langle V_n(t)V_n(t+s) \rangle = 2D\delta(t-s), \quad (1.3)$$

where D is the noise intensity.

Equation (1.1) represents a bistable potential whose barrier height in the absence of modulation, $c \equiv 0$, is $\Delta U = a^2/4b$ and where the potential minima are located at $x_0 = \pm\sqrt{a/b}$. When $c > 0$, the potential is "tipped" at the modulation frequency such that each potential minimum is alternately raised and lowered relative to the barrier height. Bistability is destroyed for $c \geq (4a^3/27b)^{1/2}$, and in this and all referenced works only the bistable regime is considered.

The phenomenon of stochastic resonance can be understood as follows: When the classical dynamics is confined to the bistable regime, and when the noise is zero, no switching between minima is possible. The state of the system will be confined to one well or the other depending on initial conditions. If we define the output signal to be one or more switching events, then for $V_n = 0$ no signal appears at the output. It is important to note, howev-

er, that $x(t) \neq 0$ or a constant in this case. Because the modulation also induces a periodic variation at the same frequency in the location of the potential minima, the response of the deterministic system, i.e., the solution of Eq. (1.2) with $V_n = 0$, will be of the form

$$x_0(t) = \epsilon \sin(\omega_m t + \phi) + h, \quad (1.4)$$

where h represents higher harmonics, ϵ and ϕ are normally small (compared to a , b , c , and 2π) but depend on these parameters and ω_m , and where $x_0(t)$ is confined to the close neighborhood of one or the other minimum. This "zero noise" dynamics is not the main interest here but will be necessary later. Instead, we note that for $V_n > 0$ there will always be noise-induced switching at some rate. Thus an increase in the noise intensity results in an increased switching rate. In the absence of modulation, the switching rate is given by the well-known Kramers formula¹⁴

$$R = \frac{a}{\pi\sqrt{2}} \exp \left[- \frac{2\Delta U}{D} \right]. \quad (1.5)$$

With modulation, ΔU becomes a time-dependent quantity $\Delta U \rightarrow \Delta U_0 + u \sin(\omega_m t)$. Therefore the switching rate becomes modulated at the frequency ω_m . The output signal is therefore correlated with the noisy modulation, or input signal, and this correlation has been induced *purely* by the additive noise.¹⁵ The power spectrum of the output therefore shows a strong peak at the modulation frequency. In this and previous work, the SNR of the output is defined as the ratio of the maximum amplitude of this peak to the amplitude of the noise background at the signal frequency ω_m . It is easy to intuit then that increasing the noise intensity at the input, i.e., decreasing the input SNR, leads to a larger SNR at the output. This is true only over a limited range. With increasing noise intensity the output SNR passes through a maximum, and for higher levels of noise, the correlation between input and output becomes increasingly washed out. The maximum SNR evidently occurs when the noise-intensity-dependent escape time, averaged over the changing potential, becomes comparable to the half period of the modulation. This behavior has given rise to the somewhat misleading term *resonance*.

In this paper, we present the results of an analog simulation of Eqs. (1.1) and (1.2) in the form of high-resolution measurements of the power spectrum, from which the SNR's are obtained, and the probability density of residence times. Because our resolution is higher than previously reported digital or analog simulations, we are able to test unequivocally certain predictions of the theory as outlined below. In particular, we observe (i) a very clear sequence of peaks in the power spectrum at odd multiples of the modulation frequency; (ii) a similar sequence of peaks in the probability density of residence times located at odd integer multiples of the half period; (iii) the appearance of a sequence of peaks at even integer multiples of the modulation frequency when the symmetry of the unmodulated potential is destroyed; and (iv) that the total power of the noise plus the signal in the power spectrum is a constant to within a small uncertain-

ty resulting from the finite measurement bandwidth. (The last result, however, is not true for the general dynamics but only for the filtered-two-state dynamics.)

In Sec. II we review the main results of the modern theories.⁷⁻¹¹ In Sec. III we briefly review the analog simulation technique, outline those modifications specific to this simulation, and display some sample data. Section IV presents our tests of the main theoretical predictions, in particular, the two predictions [see items (a) and (b) in Sec. II below] which have not yet been tested experimentally or in any simulation. In addition, we present some data on colored noise for which a recent theoretical estimate and a simulation has been given in Ref. 12(b). Finally, we make some concluding remarks in Sec. V.

II. SUMMARY OF PREDICTED RESULTS

The challenge for theorists is that Eq. (1.2) cannot be solved exactly because the potential is not time independent, and hence the probability densities are not stationary. Standard Fokker-Planck techniques for obtaining the probability flows of one-dimensional systems cannot be used, and consequently the Kramers formula no longer gives quantitative values for the transition rates. An obvious approach is to make an adiabatic approximation by restricting the modulation frequency to low enough values that the potential changes only quasistatically. This means that the modulation frequency must be small compared to the unmodulated Kramers rate, or $\omega_m \ll R$, and the probability densities are then assumed to be quasistationary. This general approach was originally elucidated by Caroli *et al.*¹⁶ and first applied to the stochastic resonance problem, specifically to the ice-age model, by Nicolis.¹⁷ Later applications of the adiabatic technique to modulated bistable systems¹⁸ and specifically to the stochastic resonance problem have been given by McNamara and Wiesenfeld⁷ and by Marchesoni and his co-workers.¹¹ The adiabatic approximation has been avoided by an essentially two-dimensional theory due to Jung and Hänggi⁸ and Jung.¹⁰ We briefly outline here the main predictions of the two modern theories only.

The main results of the adiabatic theories can be summarized as follows: (i) The power spectrum consists of two parts: a Lorentzian noise background centered on $\omega=0$ and a single δ function located at ω_m contributed by the signal; and (ii) the sum of the total powers in the signal and the noise is a constant. Thus increasing the signal power input results in an increase in the signal power output accompanied by an equal decrease in the output noise power.

A hint of this latter remarkable result, obtained analytically in the McNamara-Wiesenfeld two-state theory, was also found earlier in the data of Fauve and Heslot. A formula for the SNR is obtained, which, except for the largest noise levels, is well approximated by

$$\mathcal{R} \cong \left[\frac{Q}{D^2} \right] \exp \left[-\frac{2\Delta U}{D} \right], \quad (2.1)$$

where

$$Q = ax_0^2 c^2 \sqrt{2} \quad (2.2)$$

and \mathcal{R} represents the SNR.

An essentially two-dimensional approach to the Fokker-Planck equation analogous to Eqs. (1.2) and (1.3), which avoids the necessity of making an adiabatic approximation, has been realized by introducing the time-dependent phase $\phi(t)$ into Eq. (1.2), which now reads^{8,10}

$$\dot{x} = ax - bx^3 + c \sin[\omega_m t + \phi(t)] + V_n(t), \quad (2.3)$$

where $\phi(t)$ is a random function, uniformly distributed on $[0, 2\pi]$ with density $(2\pi)^{-1}$. Following the techniques developed in Ref. 14(a), a two-dimensional, stationary probability density $W_{st}(x, \theta)$, with $\theta = \omega_m t + \phi(t)$, was obtained from matrix continued fraction expansions. Two specific predictions are of interest here: (a) The asymptotic autocorrelation function of the output $x(t)$ contains undamped oscillations,

$$S(\tau \rightarrow \infty) = \langle x \rangle^2 + \sum_{n=1}^{\infty} \alpha_n \cos(n\omega_m \tau), \quad (2.4)$$

at integer multiples of the modulation frequency. This implies, via the Wiener-Khinchine theorem, that the power spectrum, and hence the SNR, of the output must contain δ functions;¹⁹ and (b) the even numbered coefficients α_n vanish, so that a sequence of δ functions are to be expected only at *odd* multiples of ω_m .

III. SIMULATOR AND EXAMPLE DATA

The principles of our analog simulations have been previously reviewed in Ref. 14(b), Vol. 3, and therefore will not be reiterated here. The construction of an analog model of Eqs. (1.1)–(1.3) is straightforward. The only special consideration is related to the stability of the signal generator for the modulation term in Eqs. (1.1) and (1.2). We have mentioned before that the width of a frequency bin in the measured power spectrum is determined by the bandwidth of the measurement apparatus, and further that drifts in the frequency of the modulating signal generator comparable to the width of a bin can lead to large errors in determinations of the signal amplitude.¹³ This effect, called the “scalping loss,” was also discussed by McNamara and Wiesenfeld.⁷ In order to overcome this limitation, we used a precision frequency synthesizer (Comstron, model 1013) with a resolution of 0.1 Hz and a stability of less than 1 part in 10^8 per day. We found that the signal peak in the power spectrum was then always confined to a single bin. The amplitude of the signal peak was therefore determined solely by the bandwidth of the measuring apparatus, which was constant throughout the simulation. The measured SNR data shown below exhibit considerably less scatter than either those we previously reported in Ref. 13 or the data from the laser experiment of Ref. 6. In the case of our simulations, this improvement was the result of replacing the ordinary signal generator with the synthesizer.

Fluctuating output voltages from the electronic circuit simulating $x(t)$ in Eq. (1.2) were digitized with an analog-to-digital converter board (Data Translation, model 2821-G) in a PC-AT computer. Using Asyst

software, the digitized data were fast-Fourier transformed and the resulting power spectral densities were averaged. Depending on the application typically 10 to 40 million digitized data points were assembled into the final results. The power spectra were measured by digitizing either 2048 or 4096 points of $x(t)$ into a time series, then pausing to calculate the transform and do the averaging, then opening the digitizer to obtain the next sample of $x(t)$. As many as 10 000 such samples contributed to the final average. We have also made high-resolution measurements of the probability density of residence, or "sojourn," times, that is, the times between barrier-crossing events which mark the entrances and escapes from a single well. As shown below, this quantity, like the power spectrum, is also very sensitive to correlations between the output and the modulation and hence is complimentary to it.

In this experiment, we set the well parameters $a=b=1.0$ for simplicity and so that our $x(t)$ output would range around ± 1 V. The unmodulated barrier height was then $\Delta U = \frac{1}{4}$, with the potential minima located at ± 1 V. The simulator was operated over a 50-kHz bandwidth with a characteristic time (the integrator time constant) of $\tau_i = 1.0$ ms. In order to simulate white noise, the output of our 200-kHz bandwidth, Gaussian noise generator (Quan-Tech, model 420) was passed through a linear filter with a time constant of $\tau_n = 100 \mu\text{s}$, then applied to the circuit. The dimensionless noise correlation time was thus $\tau = \tau_n / \tau_i \cong 0.10$ for most of the results presented below. The noise correlation function after filtering is

$$\langle V_n(t)V_n(t+s) \rangle = \left[\frac{D}{\tau} \right] \exp(-|t-s|/\tau), \quad (3.1)$$

which for $t \rightarrow s$ becomes $D = \tau \langle V_n^2 \rangle$. Since the mean-square noise voltage after filtering is a measured quantity, this formula serves to define the experimental values of the noise intensity D . Electronic simulators are not, however, as quantitatively accurate near the white-noise limit as compared to their accuracy at longer correlation times. Specifically, our measured values of D are always underestimates caused by clipping of the wings of the Gaussian noise by the finite range (± 10 V) of the electronics, an effect which becomes more pronounced as $\tau \rightarrow 0$. No attempt has been made here to correct for this inaccuracy.

An example digitized time series $x(t)$ is shown in Fig. 1(a) for $\sqrt{D} = 0.127$ V, which is somewhat below the resonance condition $(D_{\text{res}})^{1/2} \cong 0.3$ V. Noisy motion within the wells (intrawell motion) located near ± 1.0 V and noise-induced switching between wells is evident. What is not so evident in Fig. 1(a) is that a significant harmonic component at the modulation frequency is contained in the intrawell motion as mentioned in Sec. II. In the limit as $D \rightarrow 0$, this motion becomes dominant and, since the switching rate between wells approaches zero, it represents the largest contribution to the SNR. None of the contemporary theories take into account the intrawell motion, though McNamara has made a workable model.²⁰ In order to be comparable to the theory, the simula-

tor must therefore eliminate the intrawell motion. We accomplished this by passing the output of the simulator through a comparator circuit which executed the following logic: comparator output is ± 1.0 V for $x(t) \geq 0$. Since the barrier maximum is located at $x = 0$ V, the comparator state is changed only on barrier-crossing events, and consequently its output should approximate the filtered two-state model. A digitized sample of the comparator output is shown in Fig. 1(b). In the sequel,

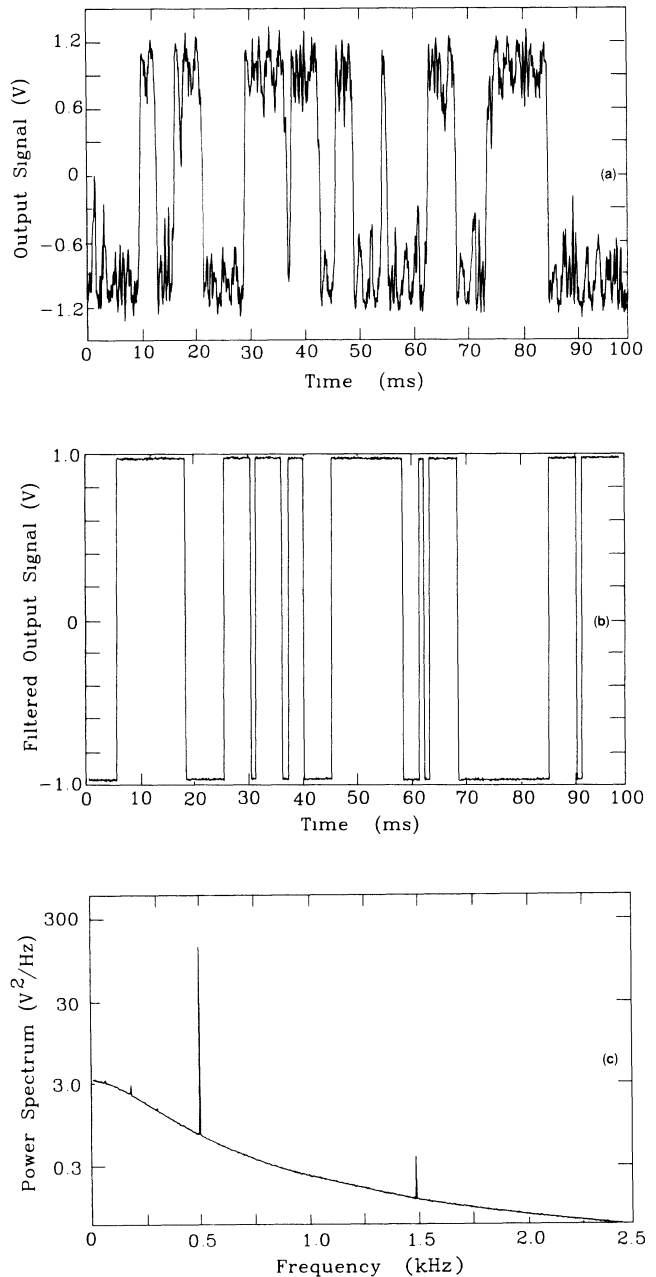


FIG. 1. (a) A measured time series from the analog simulator of Eqs. (1.1)–(1.3). (b) A measured time series from the simulator of the filtered two-state dynamics. All intrawell motions have been filtered out, leaving only the barrier-crossing transitions. (c) A measured power spectrum for $F_m = 500$ Hz, $D = 0.1$ V², and $c = 0.35$ V.

the power spectra were always obtained from the comparator outputs. The resulting SNR's approach zero, instead of infinity, when $D \rightarrow 0$. An example power spectrum is shown in Fig. 1(c). Note that the vertical scale is logarithmic, and the units are V^2/Hz . This represents the true power spectral density of the output voltage if it were dissipated in a $1\text{-}\Omega$ resistor. This power spectrum shows a strong peak at the modulation frequency ω_m , in this case 500 Hz, and a weaker peak at $3\omega_m \cong 1.5$ kHz superimposed on a Lorentzian noise background. Small peaks at the power line frequency and its fifth harmonic, and a somewhat stronger one at its third harmonic, are also evident. As we show below, the amplification of odd harmonics is a signature of the stochastic resonance system.

The SNR's were obtained by extracting the amplitudes of the fundamental signal peak S and the noise background N at the frequency ω_m from the measured power spectra. Since we used the ultrastable frequency synthesizer, the complete signal feature is located within one bin of width Δ in the power spectrum, and its amplitude represents the total signal power, unlike the noise power which is distributed over the entire bandwidth. In these simulations, Δ was usually 1 or 2 Hz. The ratio $R = (S + N)/N$ was formed, and the value of R in decibels was defined as the SNR

$$\mathcal{R} = 10 \log_{10} R . \quad (3.2)$$

Figure 2 shows the result of this data reduction procedure where the SNR and the noise N are separately plotted versus D . The asterisks are our measured results for $\Delta = 1$ Hz, $c = 0.35$, $f_m = 498.0$ Hz, and $\tau = 0.1$. The solid line is a fit of Eq. (2.1) to the data with $Q = 60.1$ $V^4 s^2$, $\Delta U = 0.054$ V^2 , and with D replaced by $D_0 + D$, where $D_0 = 0.224$ V^2 presumably represents an unaccounted-for internal noise²¹ (a correction which the authors of Ref. 6 also found necessary). In spite of this, the qualitative agreement with the theory is satisfactory. We have tested this relation before¹³ and so will not further examine the SNR's here except to present some data for colored noise in the next section.

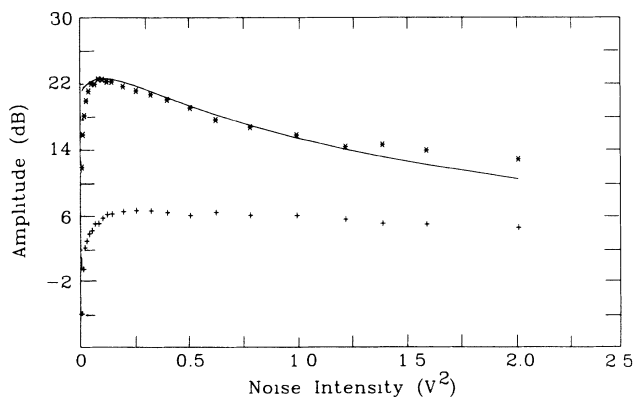


FIG. 2. The measured signal-to-noise ratio (SNR) shown by the asterisks and the noise alone shown by the plus signs in decibels as a function of the noise intensity D . The solid curve is the theory of Ref. 7 as given by Eq. (2.1).

IV. RESULTS OF THE SIMULATION

The theory outlined in Sec. II makes some interesting predictions, especially regarding the appearance of peaks in the power spectrum at odd harmonics of the modulation frequency, and the constancy of the total output power in the presence of increasing input signal power. In this section we present data which support these predictions and the results of some measurements for which no theory currently exists.

Figure 3(a) shows a power spectrum measured for a relatively low modulation frequency $f_m = 49.8$ Hz and high noise intensity $D = 0.1$ V^2 . The predicted sequence of peaks at odd multiples of f_m is clearly evident up to $5f_m$. The usual small spikes at the power line frequency and its second harmonic are also evident. There is also a very small peak at $2f_m \cong 100$ Hz which, as we shall show later, is probably caused by a small residual asymmetry in the unmodulated potential. The sequences at odd multiples persist also for larger frequencies as shown by Fig. 3(b) for $f_m = 400$ Hz. In both cases, the modulation amplitude was $c = 0.35$ V, which is very close to the critical value of $c = 0.385$ V which destroys bistability. We have observed that the higher odd-harmonic peaks decrease rapidly as c is decreased. McNamara and Wiesenfeld did not see the higher harmonics in their digital simulations, we suspect, because they only simulated small values of c . Their theory is, after all, based on an expansion of the interwell transition rate in terms of a small parameter, the leading term of which is just the modulation $c \sin(\omega_m t)$. A small peak at $3f_m$ is, however, clearly visible in the digital simulations of the laser equations of Vemuri and Roy, as shown in their Fig. 6(b) of Ref. 6(b). Moreover, this harmonic may also be present in their measurements on the actual laser, as shown on their Fig. 2(b) of Ref. 6(a). In both the digital simulations and the actual experiment on the laser system there was a larger peak at the second harmonic. We show below that this can result from an asymmetric potential. Figure 3(b), which was measured at a low noise intensity $D = 0.012$ V^2 also shows a small dip at $2f_m$. This dip was only present for relatively small noise intensities. It persists also at low frequency when f_m is 50 Hz. In some spectra, a very small dip could also be observed at $4f_m$. These dips were never observed in the spectra of the noise alone and were not evident in our stochastic resonance simulations at higher noise intensities. Figure 3(b) also shows small unexplained peaks near 600 Hz and 1 kHz.

We now consider the effect of destroying the symmetry of the unmodulated potential by adding a term βx to the potential, with $\beta \cong 0.2$. We show the resulting asymmetry with a measurement of the stationary probability density $P(x)$, of the unmodulated potential. Figure 4(a) shows the result for $D = 0.1$ V^2 . The well near $x = -1$ has become the most probable. Figure 4(b) shows the measured power spectrum for all the same conditions, except that we have switched on the modulation with frequency $f_m \cong 50$ Hz and amplitude $a = 0.35$ V. Now smaller peaks at the even multiples near 100 and 200 Hz have appeared. This might explain the observed even harmonics in the laser experiment; however, it is also

possible that they result from multiplicative modulation of the barrier height as elaborated by Marchesoni and co-workers¹¹ and as suggested by our earlier simulation with combinations of multiplicative and additive modulation and noise.¹³

Sequences of maxima also appear in the probability density of residence times. The residence times T_r are defined here as the times spent in one well (say the posi-

tive one) as shown on Fig. 1(b). In the absence of modulation, time series measured after the comparator, described in Sec. III, are accurate approximations of the random telegraph signal, for which the probability density of residence times is an exponential,

$$P_{\text{rand}}(T_r) = \langle T_r \rangle^{-1} \exp(-t/\langle T_r \rangle). \quad (4.1)$$

However, in the presence of modulation $P(T_r)$ becomes

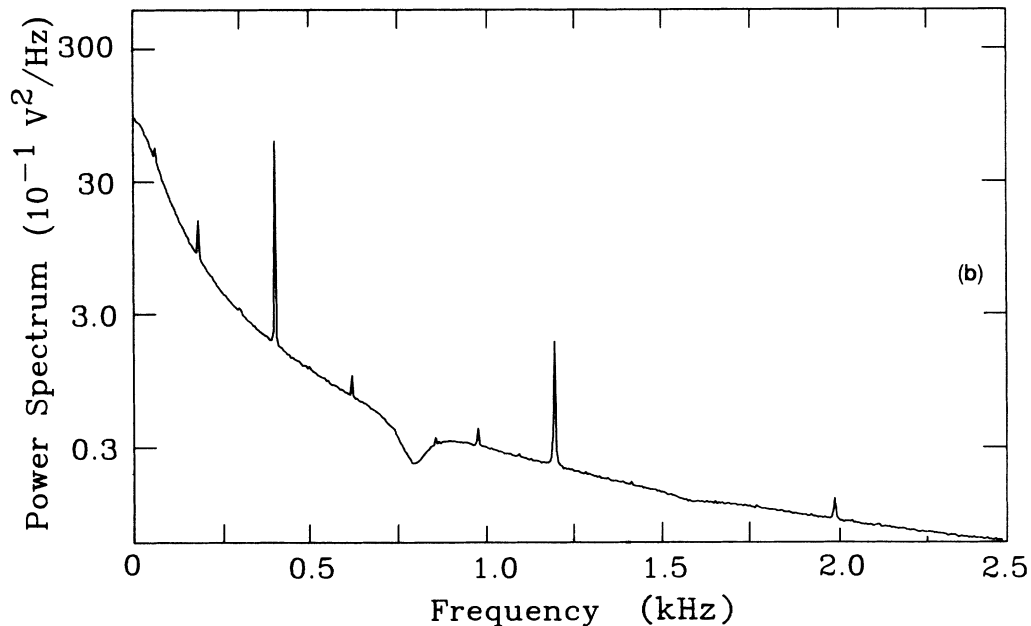
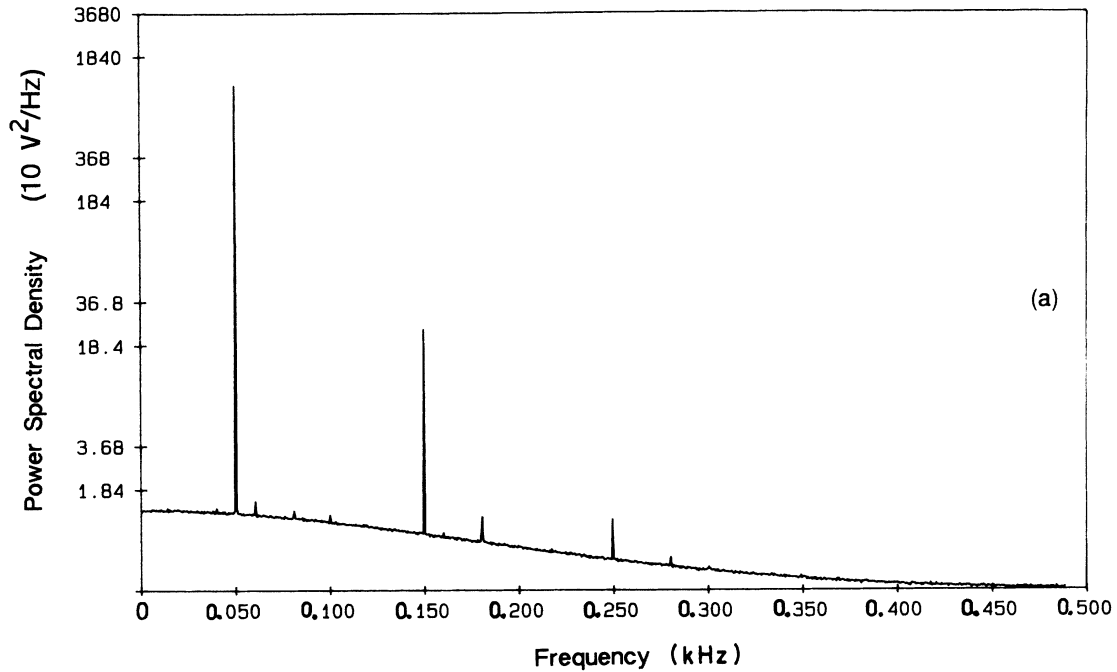


FIG. 3. (a) A power spectrum showing the sequence of peaks at odd multiples of the fundamental frequency $f_m = 49.8$ Hz for $D = 0.1$ V² and $c = 0.35$ V. (b) A power spectrum for smaller noise intensity $D = 0.012$ V² and higher frequency $f_m = 400$ Hz showing the odd-harmonic behavior plus an unexplained dip at $2f_m$.

highly structured with well-defined peaks located at odd multiples of the half period of the modulation. We show an example in Fig. 5(a) obtained at a modulation frequency $f_m = 500$ Hz ($T_m/2 = 1$ ms) from 40 million digitized points (10^4 samples of 4096 points each). Ten such peaks are easily visible. The same data are replotted in Fig. 4(b) on a logarithmic scale, where the dashed straight line shows an exponential dependence on time of the maxima. The measured characteristic time for this decay is 1.01

ms, which can be compared to the modulation half period of 1.0 ms ($f_m = 500$ Hz) and to $\langle T_r \rangle$, which from Fig. 4(a) is approximately 1 ms. Further analysis of the properties of this decay law are in progress here.

There is no theory which can predict the shape of $P(T_r)$ at present, however, the detailed structure shown in Fig. 4 suggests that this quantity may be an interesting alternative to the power spectrum for characterizing stochastic resonance. Certainly, the odd multiple structure

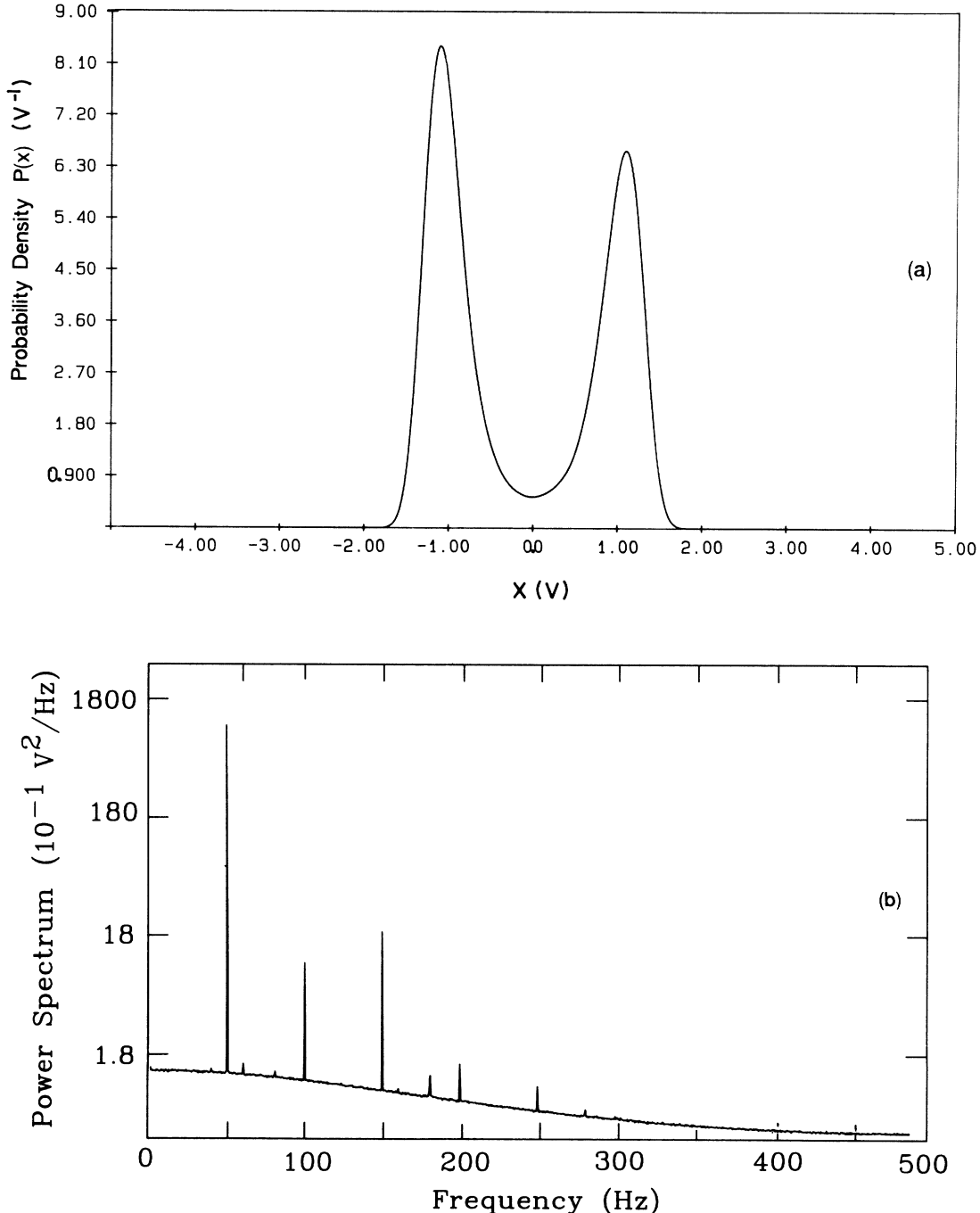


FIG. 4. (a) The stationary probability density $P(x)$ of the unmodulated potential with destroyed symmetry. (b) The power spectrum of the asymmetric potential for $D = 0.1$ V² and $f_m = 49.8$ Hz showing the even harmonics induced by the asymmetry.

reflects a basic symmetry of the dynamics: if, near the appropriate maximum in the modulation, a transition from, say, well A to well B occurs, and the reverse transition $B \rightarrow A$ does not take place at the next most probable opportunity one half period later, then the system must await one complete period of the modulation for the next most probable opportunity for a $B \rightarrow A$ transition. A total time equal to $3T_m/2$ would have elapsed commencing

at the original $A \rightarrow B$ transition. While problems involving information flow in the presence of noise have traditionally been studied by means of power spectra, other applications, for example, the ice-age model, might be better formulated in terms of the probability density of residence times.

The odd multiple structure of $P(T_r)$ leads one to speculate on the relationship, if any, between $P(T_r)$ and

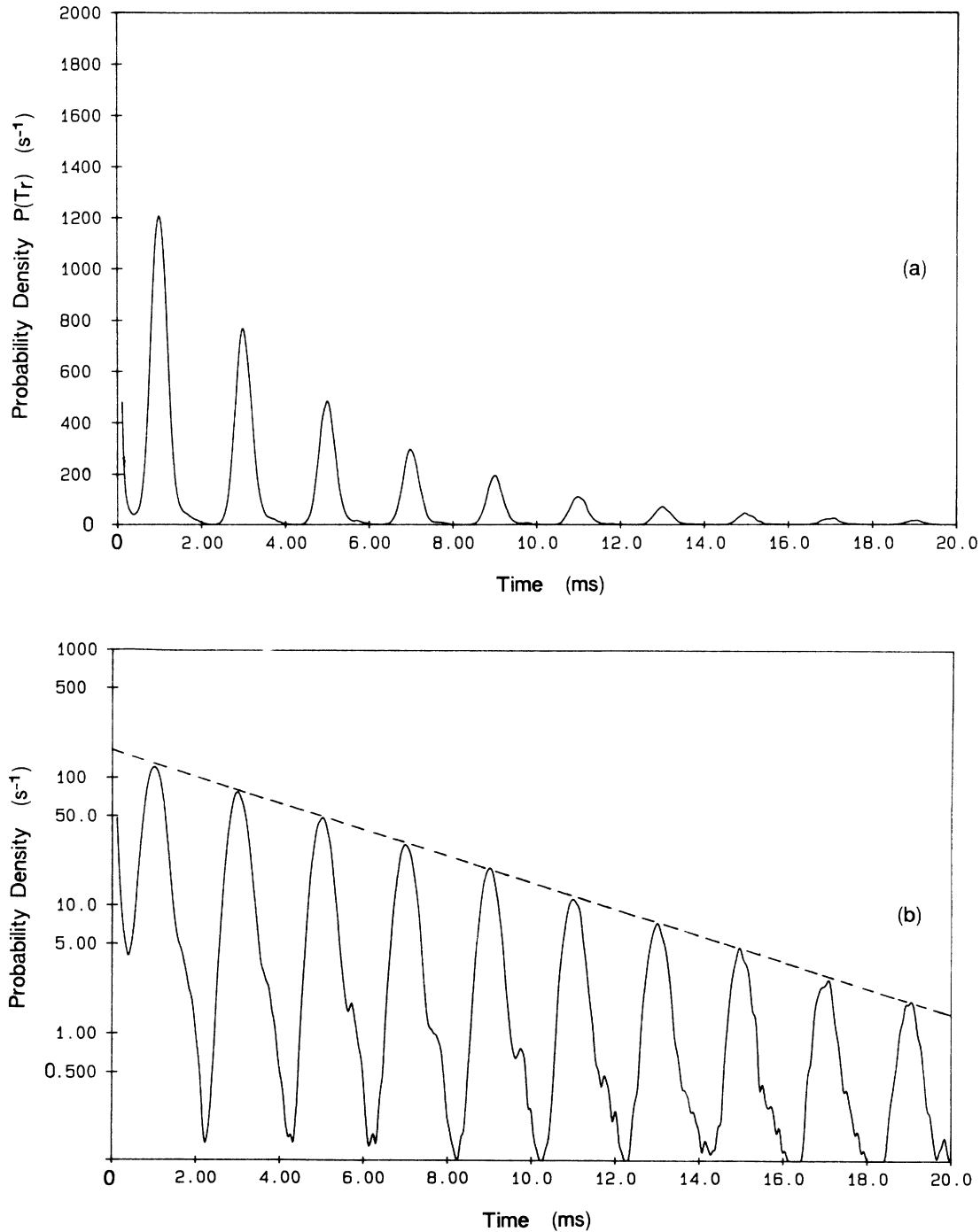


FIG. 5. (a) A high-resolution measurement of the probability density of residence times $P(T_r)$ for $D = 0.016 \text{ V}^2$ and $f_m = 500 \text{ Hz}$ showing a sequence of maxima at odd multiples of the modulation half period. (b) The same data as displayed in (a) replotted on a logarithmic vertical scale showing the exponential decrease in amplitude of the successive maxima.

$P(\omega)$. In particular, we might expect some feature in the power spectrum corresponding to, say, the second peak in $P(T_r)$ with its maximum at $T_r \cong 3$ ms. Since the residence time is half the period, the frequency corresponding to $T_r = 3$ ms is $f_m/3 \cong 166.6$ Hz. We have been unable to observe any such feature after careful searches at various modulation frequencies and noise intensities. See, for example, Fig. 1(c), measured at $f_m = 500$ Hz from 40 million points.

We turn now to the interesting prediction of the idealized two-state model regarding the output power:

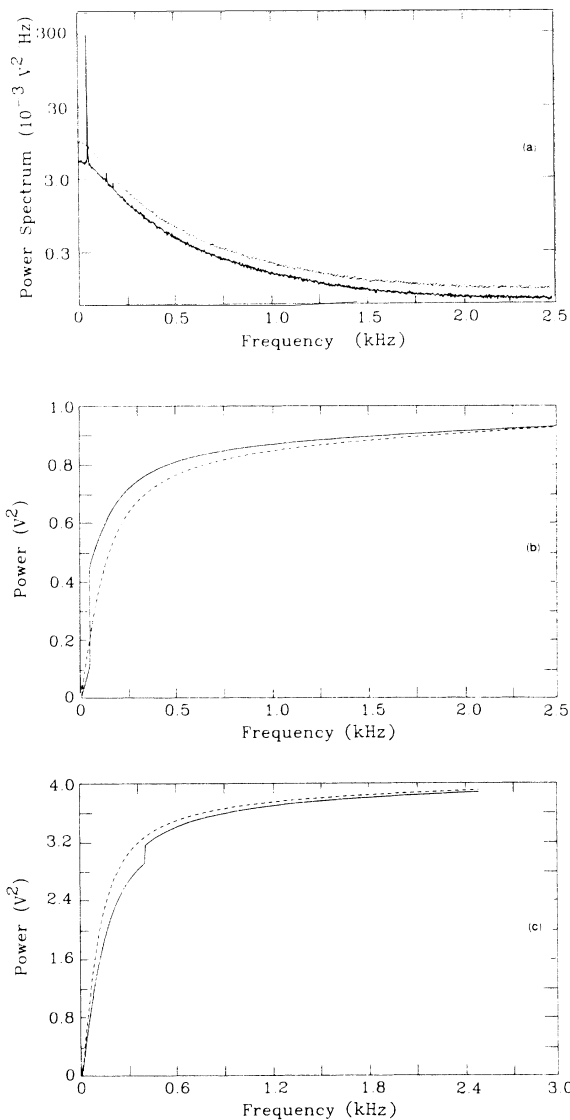


FIG. 6. (a) Two power spectra measured for $D = 0.1 \text{ V}^2$. The dotted results are the noise only ($c = 0$), and the solid curve is the same noise intensity plus the modulation with $c = 0.2 \text{ V}$ and $f_m = 49.8 \text{ Hz}$. (b) The integrals of the data shown in (a) where the noise alone is shown by the dashed curve and the noise plus modulation by the solid curve. The convergence of the two curves indicates that the total power of each of the two spectra shown in (a) is nearly equal. (c) A similar set of two integrated spectra measured for the same conditions except $f_m = 400 \text{ Hz}$.

specifically that increasing the power in the narrow-band output signal suppresses the power in the broadband noise background by an equal amount.⁷ Figure 6(a) shows a spectrum measured for $\omega_m = 49.8 \text{ Hz}$ and $D = 0.1 \text{ V}^2$ indicated by the solid line. The spectrum of the noise only, measured under the same conditions, is shown by the dotted curve. Clearly, the Lorentzian-shaped noise background is suppressed by the appearance of the signal peaks. Figure 6(b) shows the integrals of these two spectra. The noise integral is shown by the dashed curve, and the two curves converge demonstrating that the total power in the noise-plus-signal spectrum is approximately equal to that in the noise alone. They could be exactly equal only for a measurement system of infinite bandwidth. This characteristic is also preserved at higher frequencies, as shown by Fig. 6(c), for the same conditions but with $\omega_m = 400 \text{ Hz}$. Note that integration of the data does a considerable amount of smoothing. Also note that the spectral density in Fig. 6(a) is plotted on a logarithmic scale while the total power is displayed on linear scales. The amplitude of the signal spike in the density is two orders of magnitude larger than the spike at the first odd harmonic, which consequently is not visible on the scale of Fig. 6(b) or 6(c).

Finally, it is worth noting that the scales of Figs. 6(a) and 6(b) are consistent. This means that the strength $S(f)$ shown as the magnitude of the discontinuity in 6(b) is numerically related to the amplitude $P(f)$, of the peak in the density in 6(a) by $S(f_m) = P(f_m)$, since all the power is in one frequency bin. The results, used in the integral in Fig. 6(b), were obtained by fast-Fourier transforming 2048 point time series into power spectra with a frequency range of 2.5 kHz. The width of a bin was 0.456 Hz. From Fig. 6(a), $P(f_m) \cong 0.330 \text{ V}^2 \text{ Hz}^{-1}$. This compares favorably with $S(\omega_m) \cong 0.336 \text{ V}^2$ taken from 6(b). Moreover, the asymptotic value of the total power in 6(b) $P_{\text{tot}} \cong 0.92 \text{ V}^2$ is in good agreement with measurements of $\langle V^2 \rangle \cong 0.925 \text{ V}^2$ made with an ac voltmeter at the output of the circuit.

We emphasize again that the constant total power property is true only for the filtered two-state dynamics, as shown in Fig. 1(b). All the power associated with the intrawell motions, both periodic and stochastic, has been filtered out so that the only output information is contained in the barrier-crossing events. The power spectral density represented by these events is constant with the role of the modulation being simply to rearrange the crossing times by correlating them but not to alter the mean crossing rate. By contrast, Jung has demonstrated a mean-crossing-rate enhancement with increasing modulation amplitude for the full dynamics.¹⁰

Finally, we present some data on the measured SNR's for colored noise. In this case the experiment was performed exactly as before, except that the dimensionless noise correlation time was increased. Figure 7 shows some data measured for three values of $\tau = 0.1, 1, \text{ and } 4$. We note that simply increasing τ leads to more rounding of the graph and a shifting of the maxima toward larger noise intensities. We have not made a detailed analysis of these data, but note that they are in good qualitative agreement with both theoretical and experimental results

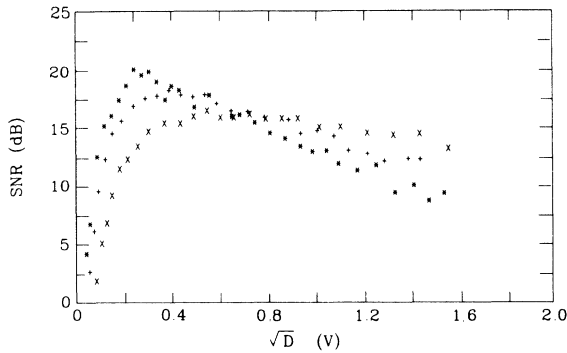


FIG. 7. Measured SNR's for various noise correlation times plotted vs the square root of the noise intensity. The asterisks are for $\tau=0.1$, or quasi white noise; the plus signs for $\tau=1.0$; and the crosses for $\tau=4.0$.

obtained by Marchesoni and co-workers, as given in Ref. 12(b).

V. SUMMARY

We conclude by noting that for the filtered two-state stochastic resonance system, we have observed the dom-

inant features predicted by the two recent theories: those based on the adiabatic approximation and the two-dimensional generalization with matrix-continued fraction solutions. We have observed the property that the total power in the output is a constant independent of modulation amplitude as predicted by the former, and the sequence of peaks in the power spectra at odd multiples of the modulation frequency predicted by the latter. In addition, we have shown that peaks at even multiples result when the unmodulated symmetry of the potential is destroyed. Finally, we have introduced high-resolution measurements of the probability density of residence times as an alternative to the power spectrum for characterizing stochastic resonance.

ACKNOWLEDGMENTS

We are grateful to Grigorie Nicolis, Peter Jung, Peter Hänggi, and Fabio Marchesoni for valuable discussions. This work was supported by the U.S. Office of Naval Research Grant No. N00014-88-K-0084 and by NATO Grant No. 0770/85.

*Permanent address: Institute for Semiconductors, Chinese Academy of Sciences, Beijing, People's Republic of China.

¹R. Benzi, S. Sutera, and A. Vulpiani, *J. Phys. A* **14**, L453 (1981).

²C. Nicolis and G. Nicolis, *Tellus* **33**, 225 (1981).

³R. Benzi, G. Parisi, A. Sutera, and A. Vulpiani, *Tellus* **34**, 11 (1982).

⁴See, for example, M. Ghil and S. Childress, *Topics in Geophysical Fluid Dynamics: Atmospheric Dynamics, Dynamo Theory and Climate Dynamics* (Springer-Verlag, New York, 1987), p. 335.

⁵S. Fauve and F. Heslot, *Phys. Lett.* **97A**, 5 (1983).

⁶(a) B. McNamara, K. Wiesenfeld, and R. Roy, *Phys. Rev. Lett.* **60**, 2626 (1988); (b) G. Vemuri and R. Roy, *Phys. Rev. A* **39**, 4668 (1989).

⁷B. McNamara and K. Wiesenfeld, *Phys. Rev. A* **39**, 4854 (1989).

⁸P. Jung and P. Hänggi, *Europhys. Lett.* **8**, 505 (1989).

⁹R. Fox, *Phys. Rev. A* **39**, 4148 (1989).

¹⁰P. Jung, *Z. Phys. B* **76**, 521 (1989).

¹¹C. Presilla, F. Marchesoni, and L. Gammaitoni, *Phys. Rev. A* **40**, 2105 (1989).

¹²(a) L. Gammaitoni, F. Marchesoni, E. Menichella-Saetta, and S. Santucci, *Phys. Rev. Lett.* **62**, 349 (1989); (b) L. Gammaitoni, E. Menichella-Saetta, S. Santucci, F. Marchesoni, and C. Presilla, *Phys. Rev. A* **40**, 2114 (1989).

¹³G. Debnath, T. Zhou, and F. Moss, *Phys. Rev. A* **39**, 4323 (1989).

¹⁴(a) For a general discussion see, for example, H. Risken, *The*

Fokker Planck Equation (Springer-Verlag, Berlin, 1989); (b) for a collection of reviews, see *Noise in Nonlinear Dynamical Systems*, edited by F. Moss and P. V. E. McClintock (Cambridge University Press, Cambridge, 1989), Vols. 1–3.

¹⁵The correlation exists only for additive modulation and additive noise. The barrier height alone can be modulated by letting $a \rightarrow a(t) = a_0 + c \sin(\omega_m t)$ with $c < a_0$, but there exists no net probability current between the wells. Consequently, while there is switching, no correlation between input and output signals exists. No noise-induced switching exists for purely multiplicative noise, $a \rightarrow a(t) = a_0 + V_n$. A related study on "heat-induced" probability flow is given by K. Sinha and F. Moss, *J. Stat. Phys.* **54**, 1411 (1989).

¹⁶B. Caroli, C. Caroli, B. Roulet, and D. Saint-James, *Physica A* **108**, 233 (1981).

¹⁷C. Nicolis, *Tellus* **34**, 1 (1982).

¹⁸P. Bryant, K. Wiesenfeld, and B. McNamara, *J. Appl. Phys.* **62**, 2898 (1987).

¹⁹The δ functions can be easily motivated by imagining the Fourier transform of Eq. (1.2). The transform of the nonlinear terms cannot be immediately imagined, but the modulation term stands alone and hence must contribute an additive δ function to the solution.

²⁰B. McNamara, Ph.D. dissertation, University of California at Santa Cruz, 1989 (unpublished).

²¹The value $D_0 = 0.224 \text{ V}^2$ is, however, far too large to represent the internal noise of our simulators, which typically exhibit internal noises less than 0.1 mV.